Applied Geochemistry 24 (2009) 1175–1184

Contents lists available at ScienceDirect

Applied Geochemistry

journal homepage: www.elsevier.com/locate/apgeochem

Aeration to degas CO_2, increase pH, and increase iron oxidation rates for efficient treatment of net alkaline mine drainage

C.S. Kirby *, A. Dennis, A. Kahler

Department of Geology, Bucknell University, Lewisburg, PA 17837, United States

ARTICLE INFO

Article history:
Received 30 May 2008
Accepted 27 February 2009
Available online 9 March 2009

Editorial handling by Dr. R. Fuge

ABSTRACT

Passive treatment systems for mine drainage use no energy other than gravity, but they require greater area than active treatment systems. Researchers are considering "hybrid" systems that have passive and active components for increased efficiency, especially where space limitations render passive-only technology ineffective. Flow-through reactor field experiments were conducted at two large net-alkaline anthracite mine discharges in central Pennsylvania. Assuming an Fe removal rate of 20 g m^{-2} day^{-1} and Fe loading from field data, 3.6×10^3 and 3.0×10^4 m^2 oxidation ponds would be required for the passive treatment of Site 21 and Packer 5 discharges, respectively. However, only a small area is available at each site. This paper demonstrates aeration to drive off CO_2, increase pH, and increase Fe(II) oxidation rates, enabling treatment within a small area compared to passive treatment methods, and introduces a geochemical model to accurately predict these rates as well as semi-passive treatment system sizing parameters. Both net-alkaline discharges were suboxic with a pH of ≈5.7, Fe(II) concentration of ≈16 mg L^{-1}, and low Mn and Al concentrations. Flow rates were ≈4000 L min^{-1} at Site 21 and 15,000 L min^{-1} at Packer 5. Three-h aeration experiments with flow rates scaled to a 14-L reactor resulted in pH increases from 5.7 to greater than 7, temperature increases from 12 to 22 °C, dissolved O_2 increases to saturation with respect to the atmosphere, and Fe(II) concentration decreases from 16 to <0.05 mg L^{-1}. A 17,000-L pilot-scale reactor at Site 21 produced similar results although aeration was not as complete as in the smaller reactor. Two non-aerated experiments at Site 21 with 13 and 25-h run times resulted in pH changes of ⩽0.2 and Fe(II) concentration decreases of less than 3 mg L^{-1}.

An Fe(II) oxidation model written in a differential equation solver matched the field experiments very well using field-measured pH, temperature, dissolved O_2, and initial Fe(II) concentration. The maximum oxidation rate was 1.3×10^{-4} mol L^{-1} s^{-1}. The model was modified to predict alkalinity, P_{CO2}, dissolved O_2, and pH changes based on initial conditions and aeration rate. This more complex model also fits the data well, is more predictive than the first model, and should serve as a tool for predicting pond size needed for aerated Fe(II) oxidation at the field scale without the need for field pilot studies. Iron(II) oxidation modeling of actively aerated systems predicted that a 1-m deep pond with 10 times less area than estimated for passive treatment would lower Fe(II) concentrations to less than 1 mg L^{-1} at summer and winter temperatures for both sites. The use of active aeration for treatment of CO_2-rich, net-alkaline discharges (including partially treated effluent from anoxic limestone drains) can result in considerably reduced treatment area for oxidation and may lower treatment costs, but settling of Fe hydroxides was not considered in this study. The reduced capital cost for earthmoving will need to be compared to energy and maintenance costs for aeration.

1. Introduction

1.1. Mine drainage and treatment background

Abandoned and untreated coal mine drainage laden with dissolved Fe and other metals pollutes streams worldwide. The drainage can be acidic, neutral, or alkaline (Kirby and Cravotta, 2005a), so for brevity, it is referred to as AMD, which can stand for abandoned, acidic, or alkaline mine drainage. In the past two decades, numerous methods of passive and semi-passive treatment of AMD have been developed to remove acidity and metals (e.g., Watzlaf et al., 2004). Treatment system design must be site-specific and depends on factors such as drainage chemistry and flow rate, area available for treatment, and the physical layout of area available (e.g., ability to take advantage of gravity flow, availability of power).

Many passive or semi-passive treatment systems receive AMD in which dissolved Fe is predominantly in the Fe(II) form. The primary reactions to remove Fe are oxidation of Fe(II)

* Corresponding author. Fax: +1 570 577 3031.
E-mail address: kirby@bucknell.edu (C.S. Kirby).

0883-2927/$ - see front matter © 2009 Elsevier Ltd. All rights reserved.
doi:10.1016/j.apgeochem.2009.02.028

$$Fe^{2+} + 1/4O_2 + H^+ = Fe^{3+} + 1/2H_2O, \quad (1)$$

and subsequent precipitation of Fe(III) solids

$$Fe^{3+} + 3H_2O = Fe(OH)_{3,s} + 3H^+, \quad (2)$$

where $Fe(OH)_{3,s}$ could be one of several amorphous or crystalline solids. In the absence of sufficient alkalinity, acidic mine drainage will also dissolve metals other than Fe from surrounding rocks. Such a solution will be "net acidic" and will require alkaline addition for successful treatment (Kirby and Cravotta, 2005a,b). However, if sufficient alkalinity is available, the resulting solution will be "net alkaline" and can "treat itself;" i.e., Fe and metals will be essentially removed, and the water will have pH $\geqslant$ 6.3, given sufficient time in a treatment system (Kirby and Cravotta, 2005a, b).

Net-alkaline AMD would have a positive value for its net alkalinity. If negative values for Hot Acidity (APHA, 1998) are reported (not always common practice), Kirby and Cravotta (2005b) recommend the use of

$$\text{net alkalinity} = -\text{measured Hot Acidity}_{(\text{APHA},1998)}, \quad (3)$$

or, if not,

$$\text{net alkalinity} = \text{Alkalinity}_{\text{measured}(\text{APHA},1998)} - \text{Acidity}_{\text{calculated}}, \quad (4)$$

where Acidity is calculated as

$$\text{Acidity}_{\text{calculated}}(\text{mg L}^{-1}\text{ as CaCO}_3) = 50 \cdot (10^{(3-\text{pH})} + 2 \cdot C_{Fe}/55.8 + 2 \cdot C_{Mn}/54.9 + 3 \cdot C_{Al}/27.0), \quad (5)$$

where C is dissolved concentration in mg L^{-1}.

Ground water and coal mine drainage commonly contain elevated concentrations of dissolved CO_2 in association with elevated partial pressures of CO_2 (Pco_2) of $10^{-1.5}$ to 10^{-} zone and/or underlying saturated zone (Cravotta et al., 1990; Langmuir, 1997; Rose and Cravotta, 1998). Elevated CO_2 concentrations contribute to the acidity and depress pH of AMD, but only temporarily (Kirby and Cravotta, 2005a, b); after the AMD emerges or has been sampled, the CO_2 eventually will degas until concentrations of dissolved CO_2 equilibrate with atmospheric Pco_2 of $10^{-3.4}$ atm (380 ppm v/v). The degassing of CO_2 from AMD can be accelerated by aggressive aeration (Jageman et al., 1988). Anoxic limestone drains (see e.g., Watzlaf et al., 2004), other $CaCO_3$ treatments, and natural alkalinity sources also can produce net-alkaline, CO_2-rich water.

Most alkalinity in AMD is from the species HCO_3^- (Kirby and Cravotta, 2005a, b), which reacts with H^+ to form carbonic acid. When this solution reaches the ground surface, the water is exposed to the air, and the dissolved CO_2 will degas towards equilibrium with the atmosphere. The increased pH due to CO_2 degassing is critical to the treatment of net-alkaline mine drainage because it indirectly causes the Fe(II) oxidation rate to increase

$$\frac{d[\text{Fe(II)}]}{dt} = -k[\text{Fe}(II)][O_2](a_{H^+})^{-2} \quad (6)$$

(Stumm and Morgan, 1996; Kirby et al., 1999), where [] indicates mol kg^{-1} and k is a temperature-dependent rate constant. Eq. (6) applies as long as pH remains near neutral (as it will in CO_2-depleted net-alkaline water). As the pH and oxidation rate increase, the rate of formation of Fe(III) hydroxide (Eq. (2)) is expected to increase until dissolved Fe concentrations are depleted. Although microbially-catalyzed Fe oxidation rates are important at lower pH values (e.g., Kirby et al., 1999), they do not need to be considered at near-neutral pH values. Dempsey et al. (2001) and Dietz and Dempsey (2002) have shown that catalysis by Fe hydroxide solids can be important at near-neutral pH values, but such catalysis appears not to make a major contribution to Fe oxidation rates at low Fe solid concentrations.

Aeration has long been used in active treatment because it can (1) add O_2, (2) help with mixing, and (3) degas CO_2, although treatment practitioners commonly focus only on the addition of O_2. More recently, aeration has been considered or used as a supplement to passive treatment, and attention is being given to CO_2 removal as a way to increase pH and Fe oxidation rates (Cravotta, 2007; Budeit, 2007; Means, 2007; Schmidt, 2007). Cravotta (2007) discusses an aeration approach similar to that taken in the current study for accelerating Fe(II) oxidation in net-alkaline mine water. Cravotta (2007) also uses Eq. (6) with the computer code PHREEQC (Parkhurst and Appelo, 1999) to model the kinetics of the processes involved.

1.2. This study

Flow-through reactors were used in the field to determine how well the aeration of net-alkaline mine water drives off CO_2, increases pH, and therefore increases Fe(II) oxidation rates. Two Fe oxidation models were developed. Model 1 predicts only Fe(II) concentrations and requires knowledge of several other parameters throughout the experiment. In addition to Fe(II) concentration, Model 2 predicts pH changes, consumption of alkalinity, dissolved O_2 concentration, and degassing of CO_2 based on the initial solution composition, requiring only temperature data during the experiment. The models were applied to calculate the size of aerated ponds required for Fe oxidation; this size was more than 10 times smaller than the size required for completely passive non-aerated ponds for the two mine discharges studied.

2. Methods

acker 5 discharges originate from flooded underground mines in the Western Middle Anthracite Coalfield of east central Pennsylvania, have net-alkaline effluent, and are being considered for treatment. Although numerous AMD sources with widely varying chemistry and flow rates have been documented in the anthracite region, there are a considerable number of high flow rate net-alkaline AMD sources (e.g., Cravotta and Kirby, 2004a; Cravotta, 2005; Wood, 1996; Reed et al., 1987).

2.1. Site 21 discharge

The Operation Scarlift (Gannett Fleming Corddry and Carpenter, Inc., 1972) Site 21 discharge is located along Quaker Run in Ranshaw, PA. It has a flow rate of ≈4000 L min^{-1} and accounts for 4% of the metal loading in the Shamokin Creek watershed (Cravotta and Kirby, 2004a). It originates from the Maysville mine borehole, flows horizontally out of a flooded deep mine ≈300 m through a culvert to a storm grate, then ≈10 m to Quaker Run. The drainage water is net alkaline, has low Al and Mn concentration (<0.2 and <3 mg L^{-1}, respectively), has low dissolved O_2 (DO), has high dissolved CO_2 (Cravotta and Kirby, 2004a), and virtually all Fe is Fe(II). All Site 21 experiments were done by pumping water from the storm grate.

2.2. Packer 5 discharges

The Packer 5 mine discharges in Girardville, PA emanate from a mine pool at a borehole and a breach. The combined discharge (borehole + breach) flows through an open ditch approximately 8 m wide. The metal loading at this site is higher than any individual mine discharge in the Mahonoy Creek watershed (Cravotta, 2005). All Packer 5 experiments were done at a bridge ≈400 m downstream of where the breach and borehole flows combine. Although the water chemistry is very similar to the Site 21

discharge, the Packer 5 discharge has a much higher flow rate of ≈15,000 L min^{-1} and higher alkalinity (Cravotta, 2005).

2.3. Field methods

Two aerated flow-through experiments using a 14-L Plexiglas tank (Fig. 1) were conducted at Site 21; one such experiment was conducted at Packer 5. One preliminary 13-h, non-aerated 14-L experiment, with limited data collected, was conducted at Site 21. Experiments were either naturally shaded or shaded by a canopy over the reactor to prevent direct sunlight exposure. At the start of each experiment, AMD was scooped from the source without stirring up sediment using a bucket and poured gently into the reactor tank with as little aeration as possible. Subsequently, a peristaltic pump introduced the AMD from the source into the upflow end of the reactor tank. Reactor volumes, flow conditions, average residence times (t_{res}), and experiment durations are listed in Table 1. An aquarium pump with four (eight for the second Site 21 experiment) diffuser stones was used to provide 4 L min^{-1} (8 L min^{-1} for the second Site 21 experiment) air in the upflow end of the reactor water.

A YSI™ multiparameter XLM 600 sonde was placed in the reactor tank to measure water temperature (T), pH, and DO, which were logged to a YSI™ 650 MDS. A sample for Fe(II) concentration was taken about every 10 min, filtered (0.45 μm, or 0.2 μm if analyzed in the laboratory), and acidified with concentrated HCl solution. A Hach™ DR2000 spectrophotometer was used to measure the Fe(II) concentration of the reactor water. The sample was diluted as necessary, and Hach™ 1,10 phenanthroline reagent was added with a 3-min reaction time, then analyzed using the built-in working curve to determine Fe(II) concentration. The spectrophotometer was zeroed using distilled water/reagent sample. The experiment was run until the the reactor was no longer detectable in the samples taken.

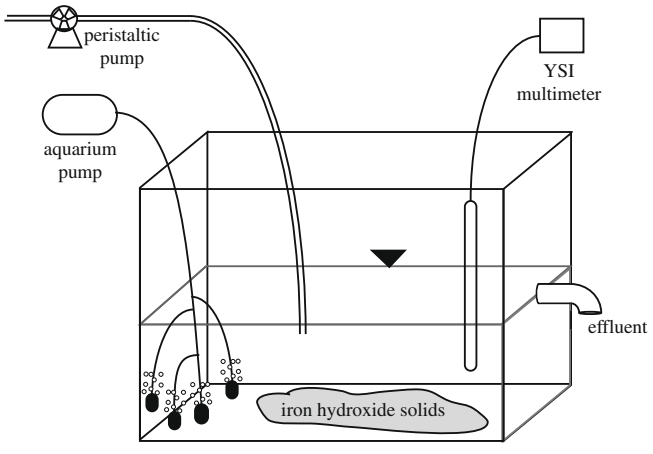

Fig. 1. Schematic diagram of 14-L flow-through reactor.

For the non-aerated Site 21 experiment, a 400-L plastic swimming pool with a flow rate of 0.33 L min^{-1} was run for 25 h. These flow conditions are scaled down from a hypothetical full-scale 1-m deep pond based on a 20 g m^{-2} d^{-1} Fe removal rate for net-alkaline passive treatment ponds (Hedin et al., 1994; Watzlaf et al., 2004). Without aeration, CO_2 degassing and therefore Fe oxidation and precipitation occur much slower, so parameters were measured less frequently than in other experiments.

For the second Site 21 14-L aeration experiment, alkalinity was measured as follows. Raw unpreserved (RU) reactor water samples (25 mL) for alkalinity were collected and titrated in the field with stirring using 0.16 N H_2SO_4 solution delivered in 1/800 mL increments from a Hach™ digital titrator to a measured pH 4.5 endpoint.

2.3.1. Pilot-scale reactor

A 17,000-L (4500-gallon) inflatable swimming pool was used as a field pilot-scale reactor at Site 21. Sump pumps introduced water from the discharge into the pool on the inflow side at 193 L min^{-1} until the reactor was full (1.5 h); experimental flow conditions are given in Table 1. Once the reactor was full, a 0.67 hp electric blower provided ambient air at 6.8 kpa (1.1 psi) to a 15-m length of Aeration Solutions, Inc. diffuser membrane in the middle of the pool. In order to examine chemical processes affected by residence time, inflow was reduced 3 h before the 26-h experiment ended. Sampling was conducted as in the 14-L reactor except that Fe(II) concentrations were approximated by analyzing filtered acidified samples for total dissolved Fe, which should be practically all Fe(II) in the pH range of the experiment (6.1–6.9).

2.4. Laboratory chemical analyses

erated 14-L Site 21 experiment, Fe(II) analyses of filtered acidified samples were conducted in the laboratory using the same methods as those used in the field. Filtered acidified samples for other metals (inductively-coupled plasma-mass spectrometry) and filtered unpreserved samples for SO_4^{2-}, Cl^-, NO_3^-, and PO_4^{3-} (colorimetric analyses) were sent to a commercial laboratory. Total dissolved and total Fe samples for the pilot-scale reactor were analyzed colorimetrically by a commercial laboratory.

2.5. PHREEQCI simulations

PHREEQCI (Parkhurst and Appelo, 1999) was used to model speciation of the influent and steady-state effluent solutions for the second Site 21 aeration experiment. Table 2 lists the major input parameters (other major ions were input to allow for charge balance) used to speciate the original solution. Table 2 also lists the changes simulated when the original speciated solution was aerated and amorphous $Fe(OH)_{3,\ s}$ was allowed to precipitate. Simulated "aeration" was accomplished by allowing equilibrium with respect to atmospheric P_{O2} and P_{CO2} using values of $10^{-0.7}$ and $10^{-3.4}$ atm, respectively. The solution was allowed to reach equilibrium with

Table 1
Reactor flow conditions. t_{res} = residence time.

Location	Reactor volume, L	Aerated?	Flowrate, L min^{-1}	Average t_{res}, h	Run time, h
Site 21	14, #1	Yes	0.028	8.3	3
Site 21[a]	14, #2	Yes	0.046 (0.023)	5.1 (10)[a]	3
Site 21	14, #3	No	0.028	8.3	13
Site 21	400	No	0.33	2.0	25
Site 21	17,000	Yes	72 (36)	3.9 (7.9)[b]	26
Packer 5	14	Yes	0.028	8.3	3

[a] Indicates flowrate reduced after 2 h.
[b] Indicates flowrate reduced after 23 h.

Table 2
Run conditions for Site 21 PHREEQCI modeling. The concentrations for other major species are not shown but were included as input.

Input	Value
Solve initial solution	
T, °C	12
pH	5.77
Alkalinity, mg L^{-1} (HCO_3^-)	117
pe	4
Fe(II), mg L^{-1}	16
Charge balance on:	SO_4^{2-}
Equilibrate with	
T, °C	22
P_{O2}, atm	$10^{-0.7}$
P_{CO2}, atm	$10^{-3.4}$; $10^{-2.42}$
Amorphous $Fe(OH)_{3,\,s}$	Saturation

respect to amorphous $Fe(OH)_{3,\,s}$. An additional simulation also used a final $P_{CO2} = 10^{-2.42}$ atm, reflective of steady-state, non-equilibrium conditions (see Section 3.2).

2.6. Iron oxidation models

Using Stella™, a graphical interface differential equation solver, the model of Kirby et al. (1999) was modified to model abiotic Fe(II) oxidation. Iron(II) oxidation in the model is governed by a temperature-dependent version of Eq. (6) (see Fig. 2). The sensitivity of Fe oxidation for this is pH > *T* > influent Fe(II) concentration >> DO > reactor volume (Kirby et al., 1999).

Model 1 is a subset (lacks the lower 3 fluxes in Fig. 2: HCO_3^-, $H_2CO_3^*$, and O_2) of Model 2. Model 1 was used for early experiments for which alkalinity was not measured. Input includes initial

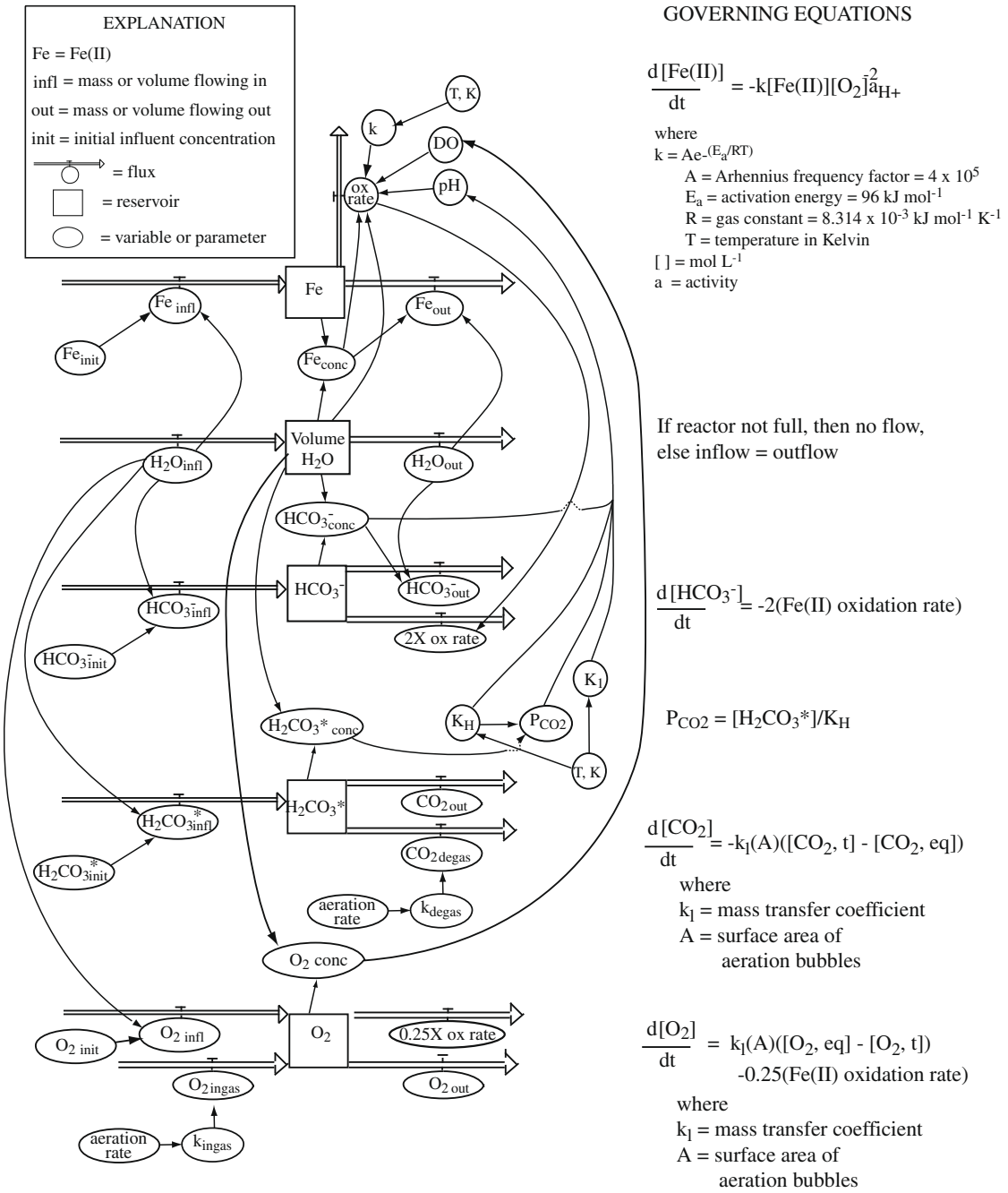

Fig. 2. Schematic diagram representing the mathematical relationships in Model 2. Arrowheads point to parameter that is a function of the parameter at the initial end.

Table 3
Equation fit parameters for the temperature-dependent equilibrium constant values for C species from the PHREEQCI database (Parkhurst and Appelo, 1999). Equilibrium constants were calculated as $\log K = A_1 + A_2T + A_3/T + A_4\log 10T + A_5/T^2$, where T is in Kelvin.

Reaction	A_1	A_2	A_3	A_4	A_5
$H_2O + CO_{2,v} = H_2CO_3^*$	108.3865	0.01985076	−6919.53	−40.45154	669365
$CO_3^{2-} + 2H^+ = H_2CO_3^*$	464.1965	0.09344813	−26986.16	−165.75951	2248628.9
$CO_3^{2-} + H^+ = HCO_3^-$	107.8871	0.03252849	−5151.79	−38.92561	563713.9

measured Fe(II) concentration and time-variant measured values for pH, DO, T, and solution flow rate. Output is the predicted Fe(II) concentration with time, which was compared to the measured Fe(II) field concentrations.

Model 2 was developed to be more widely predictive. Rather than using field data for alkalinity and pH changes, Model 2 uses only the initial field data for alkalinity, DO, pH, and calculated initial CO_2 concentration, and it then predicts alkalinity, pH, P_{CO2}, and CO_2, O_2, and Fe(II) concentrations with time, using governing equations (see also Fig. 2) as follows below.

P_{CO2} during the simulations was calculated from [$H_2CO_3^*$] and the Henry's law constant, K_H (Table 3). The initial value of P_{CO2} was calculated by PHREEQCI speciation of field pH, alkalinity (HCO_3^- concentration), and major cations and anions. The rate of CO_2 loss was calculated by mass transfer (see Fig. 2). Because an attempt to calculate k_lA_{air} for the Aeration Solutions, Inc. diffuser/blower setup based on data from the manufacturer was not successful, A_{air} and k_l were lumped together (k_lA_{air}) and used as a fit parameter. This fit was accomplished by iteratively changing k_lA_{air} until Fe(II) concentrations computed closely matched experimental values with time. The rate of O_2 gain was calculated by mass transfer (see Fig. 2). The same values for k_lA_{air} were used for CO_2 loss and O_2 gain.

Temperature-dependent equilibrium constant values from the PHREEQCI database were combined to calculate pH in Model 2, giving pH as

$$\mathrm{pH} = -\log\{K_1K_HP_{CO2}/(0.92[HCO_3^-])\} \quad (7)$$

where 0.92 is the value of the activity coefficient (calculated in PHREEQCI) for HCO_3^- for solutions in this study. Over the course of a PHREEQC aeration simulation of field solution changes in this study, the ionic strength changes only approximately 10%, thus a constant value for the activity coefficient is a reasonable approximation. The $\log K$ values (Table 3) were added to $\log K_H$, plotted in a spreadsheet and fitted to the simpler expression

$$\log(K_1K_H) = -4.233\mathrm{E}-05(T^2) + 1.887\times10^{-2}(T) - 9.682, \quad (8)$$

where T is in Kelvin.

Loss of CO_2 does not affect alkalinity directly (Stumm and Morgan, 1996; Kirby and Cravotta, 2005a), but the alkalinity decreases as Fe oxidation and hydrolysis reactions proceed:

$$Fe^{2+} + 2HCO_3^- + 1/4O_2 + 1/2H_2O = Fe(OH)_{3,s} + 2CO_{2,v}. \quad (9)$$

By the stoichiometry of Eq. (9), Model 2 assumed that 2 mol HCO_3^- were consumed by oxidation of 1 mol Fe^{2+}.

3. Results and discussion

3.1. Site 21 and packer 5 experiments and Model 1

Without aeration, chemical changes were minor because reaction rates were slow. During the preliminary 13-h, 14-L non-aerated Site 21 experiment, pH increased from 6.1 to 6.3, and the Fe(II) concentration only decreased from 16.3 to 13.8 mg L^{-1}. Despite the decrease in dissolved Fe(II) concentration, there was little visible turbidity or surface coating caused by Fe(III) precipitation.

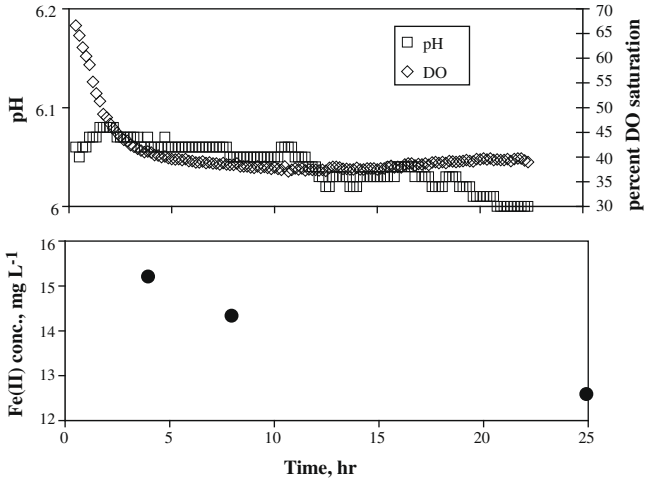

Fig. 3. Data for the Site 21 400-L non-aerated experiment.

The 400-L non-aerated Site 21 experiment ran for 25 h (Fig. 3). The pH remained constant (within analytical uncertainty). The DO apparently decreased from ≈68% to ≈40% saturation. The initially high DO may be an artifact due to introduction of mine water by pumping. The DO decrease observed cannot all be accounted for by the small amount of Fe(II) oxidation. The Fe(II) concentration only decreased from 15.2 to 12.5 mg L^{-1}. There was virtually no visible precipitate in the water or on the surface of the reactor. These results were most likely due to the very limited amount of gas exchange that occurred without aeration, thus the dissolved CO_2 and pH were maintained near initial values, and Fe(II) oxidation was much slower than aerated reactors.

Aeration produced rapid changes in solution chemistry compared to the non-aerated experiments. During the 3-h Site 21 aeration experiment, the water temperature rose from 12.2 to 19.1 °C, the pH increased from 5.7 to 7.6, the DO increased from 1.5 mg L^{-1} to 8.9 mg L^{-1} (≈100% saturation), and the Fe(II) concentration decreased from 15.8 mg L^{-1} to below the 0.03 mg L^{-1} detection limit (Fig. 4). The initially clear water in the reactor became visibly cloudy with orange precipitate within 0.5 h. The water temperature increased because it approached thermal equilibrium with ambient air. The DO increased rapidly to saturation with respect to the atmosphere, then decreased to remain in equilibrium as the water temperature increased. There were three major influences on pH change. Iron(II) oxidation (Eq. (1)) and CO_2 degassing cause pH to increase, while $Fe(OH)_{3,s}$ precipitation (Eq. (2)) causes pH to decrease. The net pH increase occurred because there was sufficient alkalinity to outweigh the effect of $Fe(OH)_{3,s}$ precipitation. Iron(II) oxidation decreased the Fe(II) concentration slowly until the pH rose; Fe(II) then decreased rapidly until the Fe(II) oxidation rate reached steady-state. Model 1 results (Fig. 4) matched the Fe(II) concentrations very well in both trend and actual values. The measured Fe(II) concentrations at steady-state were below detection limit (0.03 mg L^{-1}); model Fe(II) steady-state concentration was 0.01 mg L^{-1} (99.5% oxidation).

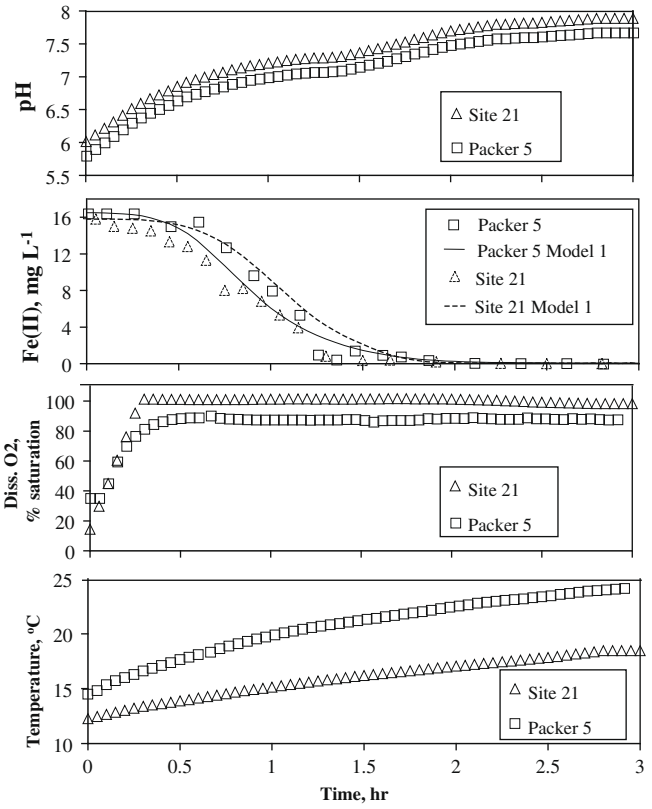

Fig. 4. Data (symbols) and Model 1 Fe(II) concentration predictions (curves) for first Site 21 and Packer 5 14-L aeration experiments.

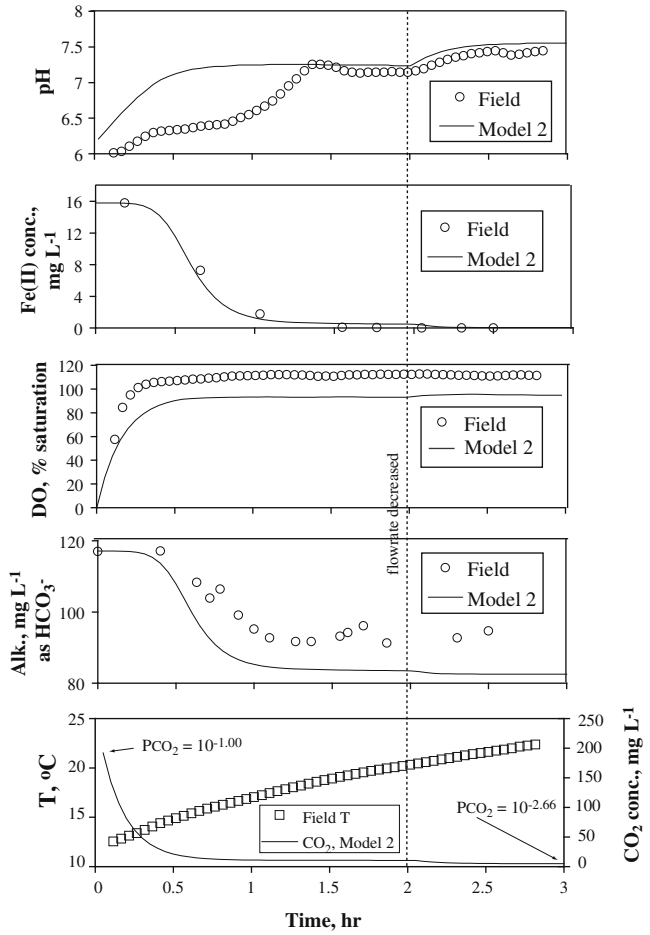

Fig. 5. Measured data (symbols) and Model 2 predictions (solid curves) results for second 14-L Site 21 aeration experiment.

For an ideally-mixed flow-through reactor, the reaction rate is calculated as

$$\text{rate} = (\text{concentration}_{\text{in}} - \text{concentration}_{\text{out}}) \times (\text{volumetric flow rate}). \quad (10)$$

The aerated reactor was not stirred and may not have been completely mixed, but the aeration did provide some mixing. Eq. (10) thus likely provides a reasonable estimate of the reaction rate The maximum oxidation rate occurred at steady-state and was 1.3×10^{-4} mol L^{-1} s^{-1}.

The 3-h Packer 5 aeration experiment yielded results similar to Site 21. The water temperature rose from 13.9 to 24.1 °C, the pH increased from 6.1 to 7.3, the DO increased from 3.7 to 7.4 (≈90% saturation) mg L^{-1}, and the Fe(II) concentration decreased from 16.5 to 0.07 mg L^{-1} (Fig. 4). The maximum oxidation rate was the same as the Site 21 rate. Model 1 results (Fig. 4) again matched the Fe(II) concentrations very well.

The results presented above and in Fig. 4 show that the aeration and the consequent removal of dissolved CO_2 in a net-alkaline water will increase pH and promote rapid Fe oxidation. Thus, the aeration of a pond treatment system would be an extremely effective method of Fe oxidation for either site studied or any other site with similar chemistry. The data show that as the aeration drove off the dissolved CO_2, the pH increased, the Fe(II) oxidized more readily, and $Fe(OH)_{3,s}$ formed rapidly compared to a non-aerated system.

3.2. Second site 21, 14-L aeration experiment and Model 2

Model 1 effectively reproduced field results, but it lacks predictive power because the changes in pH with time must be determined experimentally. Model 2 overcomes this problem by accounting for P_{CO2} and alkalinity changes in order to predict pH values. Model 2 required input values for the initial P_{CO2} and HCO_3^- concentration. The initial P_{CO2} value of $10^{-0.80}$ atm was obtained by running PHREEQCI. The initial HCO_3^- concentration was assumed to be equal to the measured 117 mg L^{-1} alkalinity as HCO_3^-.

The second Site 21 aeration experiment (Fig. 5) used an initial solution flow rate of 46 mL min^{-1}; this rate was decreased to 23 mL min^{-1} after 2 h. The steady-state pH values (1.25–2 h and 2.5–3 h) matched the measured pH well. Why the early transient-state Model 2 pH predictions are higher than the measured pH cannot be explained. Iron(II) concentration decreased slowly initially, decreased rapidly as pH increased, then decreased slowly as Fe(II) neared steady-state concentration. The Model 2 Fe(II) concentrations matched the field Fe(II) concentrations very well before and during steady-state conditions. The DO quickly rose, reaching saturation with respect to atmospheric O_2, then fell as temperature rose, maintaining this equilibrium; measured DO values slightly greater than atmospheric saturation are thought to be due to imperfect calibration. Model 2 alkalinity value trends matched measured alkalinity trends well. However, except for the initial value, measured alkalinity values were higher than predicted values (see Section 3.4 for discussion). Temperature increased throughout the experiment as the deep mine water began to equilibrate with atmospheric temperature.

It had initially been assumed that the aerated system would reach equilibrium with atmospheric P_{CO2} ($10^{-3.4}$ atm). However, Model 2 P_{CO2} values (Fig. 5; necessarily calculated rather than measured) decreased to steady-states (at different flow rates) that were

Table 4
Comparison of steady-state (or equilibrium for PHREEQCI model) values for the second Site 21 14-L end-of-experiment parameters. See Section 3.4 for discussion of alkalinity values; * indicates that the average of the last nine alkalinity measurements was used to calculate the steady-state value. NC indicates not calculated because of measure alkalinity error, nd indicates no analysis was performed for this parameter.

	Field	Model 2 Field flow rates	PHREEQCI $P_{CO2} = 10^{-2.42}$	Model 2 Flow = 2 mL min^{-1}	PHREEQCI $P_{CO2} = 10^{-3.4}$
pH	7.43	7.32	7.3	8.38	8.35
$H_2CO_3^*$, mg L^{-1}	NC	9	9	1	1
P_{CO2}, atm	NC	$10^{-2.66}$	$10^{-2.66}$	$10^{-3.4}$	$10^{-3.4}$
HCO_3^-, mg L^{-1}	nd	83	80	83	75
Alk., mg L^{-1} HCO_3^-	93*	83	82	83	82
Diss. Fe(II), mg L^{-1}	<0.03	0.01	3×10^{-13}	<0.01	3×10^{-15}
Diss. Fe(III), mg L^{-1}	nd	nd	10^{-3}	nd	10^{-5}

supersaturated. Cravotta (2007) also observed elevated steady-state P_{CO2} after prolonged aeration. Model 2 CO_2 concentrations dropped from 192 to 5 mg L^{-1} ($P_{CO2} = 10^{-1.00}$ to $10^{-2.66}$ atm) as field and Model 2 pH increased. Model 2 pH and CO_2 concentration as well as field pH had reached a steady-state before the flow rate was decreased. However, when the field flow rate was decreased (Fig. 5), field and Model 2 pH increased to a new steady-state, and Model 2 CO_2 concentration decreased to a new steady-state. This evidence strongly suggests that the system did not reach equilibrium with atmospheric P_{CO2}.

Table 4 compares field and modeled results for 7 parameters at either steady-state (experimental data and Model 2) or equilibrium (PHREEQCI) for the second Site 21 14-L aeration experiment. The Model 2 final P_{CO2} value of $10^{-2.66}$ atm is higher than atmospheric P_{CO2}. Slowing the flow rate in Model 2 from field conditions to 2 mL min^{-1} resulted in a pH of 8.38 and equilibrium with atmospheric P_{CO2} ($10^{-3.4}$ atm); these Model 2 results closely agree with PHREEQCI modeling. Fig. 5 and Table 4 results support the conclusion that the system has not reached equilibrium with atmospheric P_{CO2}. However, atmospheric equilibrium is not required for adequate treatment as long as the pH increases sufficiently to promote rapid Fe(II) oxidation, as it did in all of the 14-L aeration experiments.

3.3. Site 21 pilot-scale aeration experiment and model 2

Fig. 6 shows experimental and model results from the 17,000-L pilot-scale experiment. Aeration stopped from 14.25 to 17.5 run h (≈3–5 am) due to equipment malfunction. Model 2-predicted pH values matched the measured pH very well both in trends and actual values; in particular the Model 2 response was convincing when the aeration failed, when aeration was restored, and when flow rate was reduced (≈14, 17, and 23 h, respectively. Temperature remained nearly constant (12.1 to 13.7 °C) because of the large volume of the reactor. Iron(II) concentration initially decreased slowly, decreased rapidly as pH increased, then reached a steady-state value (interrupted by aeration failure and flow rate reduction) that indicated 79% oxidation. Predicted alkalinity values matched measured alkalinity values well. Dissolved O_2 quickly rose, but apparently reached only 80%, falling to 40%, saturation with respect to atmospheric O_2. The apparent decrease in DO as the experiment continued represents a systematic error: the DO membrane was discovered to be fouled by Fe hydroxides – it recorded values well below saturation in air-saturated water after the experiment was over. Model 2 predicted slight undersaturation (≈10%) with DO. End-of-experiment predicted CO_2 concentrations ($P_{CO2} = 10^{-2.0}$) never reached atmospheric equilibrium ($P_{CO2} = 10^{-3.4}$). As with the Model 1 results (Fig. 5), upward inflections in Model 2 predictions for pH, Fe(II), alkalinity, DO and CO_2 (Fig. 6) occur due to the decreased flow rate (increased t_{res}). Because CO_2 degassing was less effective than in the 14-L experiment, pH and DO were lower, and Fe(II) and CO_2 were higher in the pilot-scale experiment.

Dempsey et al. (2001) attribute much of the Fe oxidation in some passive treatment systems to heterogeneous Fe(II) oxidation, i.e., catalysis by Fe hydroxide solids, and Dietz and Dempsey (2002) have shown that heterogeneous Fe(II) oxidation can be significantly more rapid than homogeneous Fe(II) oxidation at pH values in the range of the experiments. However, the Dietz and Dempsey (2002) experiments required considerable amounts of Fe hydroxide solid to be present before the catalysis was evident. Total (unfiltered) Fe in the reactor was measured at the end of the pilot-scale experiment, and it was found to be 16 mg L^{-1} as Fe, which is only 2–4 mg L^{-1} higher than the two "no-recycle" (their no-added-Fe-solids control) experiments of Dietz and Dempsey (2002). The close match in this study and in Cravotta (2007) between measured and modeled Fe(II) concentrations and oxidation rates suggest that homogeneous Fe(II) oxidation (Eq. (6)) adequately models the results in these two studies. It is likely that systems with higher Fe hydroxide solid concentrations will exhibit faster Fe(II) oxidation than the present experiments.

3.4. Alkalinity measurements and modeling

Because degassing of CO_2, oxidation of Fe(II), and alkalinity consumption can take place during sample storage (Eq. (9)), mine water charged with CO_2 presents a particular problem for alkalinity measurement, making sharp endpoints difficult to obtain. Due to this difficulty, the absolute values of the Model 2 alkalinities do not match field alkalinities well. The Model 2 results, because they are based on stoichiometric relationships (Eq. (9)) probably give a better value for the overall *change* in alkalinity than the measured alkalinities. Results from PHREEQCI simulations returned the same change in alkalinities as Model 2.

3.5. Simple test for applicability of aeration

If a mine discharge is thought to be net alkaline and the major goal is to remove Fe (rather than Mn, which is more challenging to treat passively; e.g., Jacobson et al., 1999), a simple experiment can be performed to predict whether CO_2 degassing will yield a pH high enough for rapid Fe(II) oxidation. A sample of mine water can be aerated vigorously in a beaker containing a pH probe. Iron hydroxide should precipitate, and the pH should rise to a steady-state value in ≈30 min. It should be noted that neither adding H_2O_2 nor brief agitation are likely to degas CO_2 effectively (Cravotta and Kirby, 2004b). If the resulting pH is > 6.3, the water is net alkaline. At higher pH values, Fe(II) oxidation will be more rapid, and the effectiveness of aeration for treatment will increase.

3.6. Implications for treatment

Model 1 was used to predict steady-state (effluent) Fe(II) concentrations (Table 5) for hypothetical non-aerated and aerated

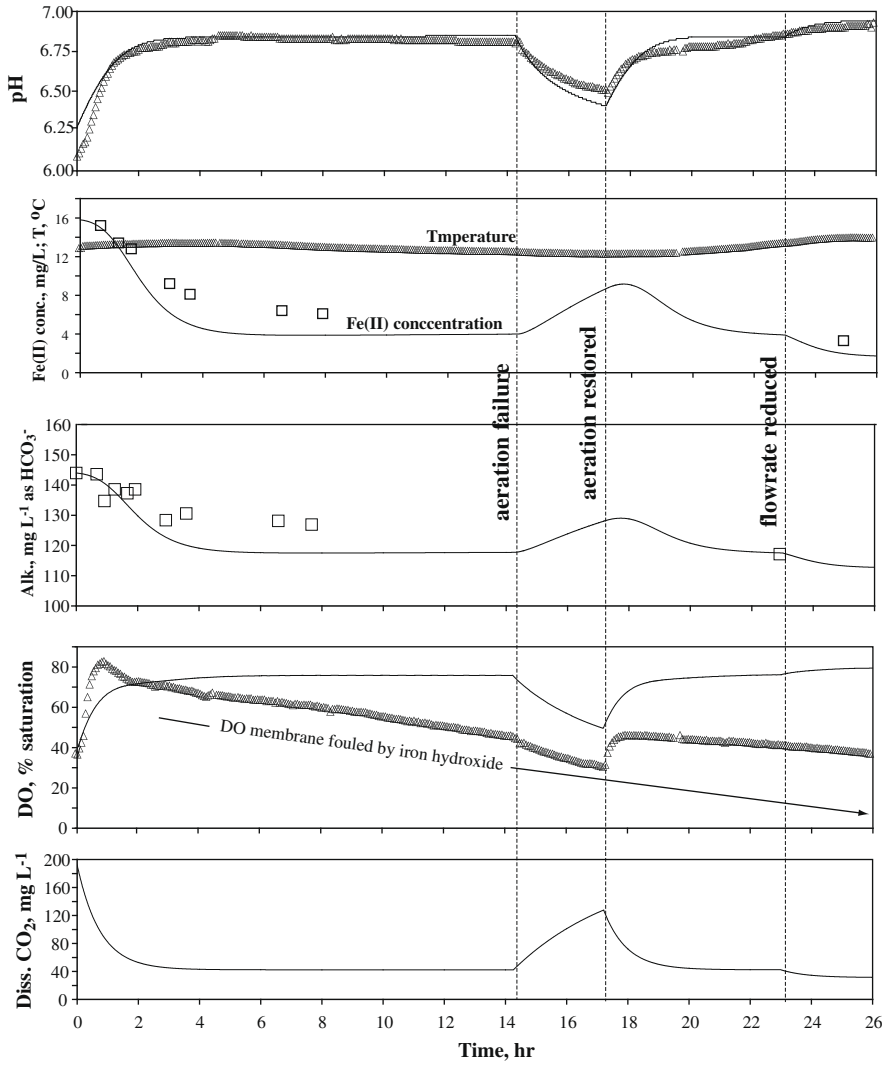

Fig. 6. Measured data (symbols) and Model 2 results (solid curves) for pilot-scale Site 21 aeration experiment.

Table 5
Model 1 predicted steady-state treatment system effluent Fe(II) concentration for aerated ponds for summer and winter conditions and a 10-fold difference in pond size. The larger pond areas are equivalent to those required using a 20 g m^{-2} d^{-1} removal rate (Hedin et al., 1994; Watzlaf et al., 2004) for passive treatment.

Site	pH	DO, mg L^{-1}	Flowrate, L h^{-1}	Pond area, m^2	Predicted Fe(II), mg L^{-1}
Summer, 25 °C					
Site 21	7.5	8	1.9×10^5	3.6×10^3	0.06
Site 21	7.5	8	1.9×10^5	3.6×10^2	0.08
Winter, 5 °C					
Site 21	7.5	12	1.9×10^5	3.6×10^3	0.6
Site 21	7.5	12	1.9×10^5	3.6×10^2	0.8
Summer, 25 °C					
Packer 5	7.4	8	1.0×10^6	3×10^4	0.01
Packer 5	7.4	8	1.0×10^6	3×10^3	0.1
Winter, 5 °C					
Packer 5	7.4	12	1.0×10^6	3×10^4	0.1
Packer 5	7.4	12	1.0×10^6	3×10^3	1.0

ponds of different sizes for the Site 21 and Packer 5 discharges (Table 5). The larger pond size for non-aerated conditions was based on a widely used Fe removal rate of 20 g m^{-2} day^{-1} (Hedin et al., 1994; Watzlaf et al., 2004), assuming that each pond was 1-m deep, and using Fe(II) loading from field data. For the same discharge, the smaller pond size for aerated conditions was one-tenth of the non-aerated size; this approach assumes that aeration is as effective as in the 14-L reactor. Note that the Hedin et al. (1994) approach predicts total Fe removal, whereas the model predicts Fe(II) oxidation without addressing Fe solid removal. Summer and winter conditions were modeled because gas equilibria, pH, and Fe(II) oxidation kinetics are all affected by temperature. For both discharges under all conditions in Table 5, predicted Fe(II) concentrations are $\leqslant 1$ mg L^{-1}, indicating that oxidation should be adequate even if treatment ponds are 10 times smaller than computed using the 20 g m^{-2} day^{-1} Fe removal rate.

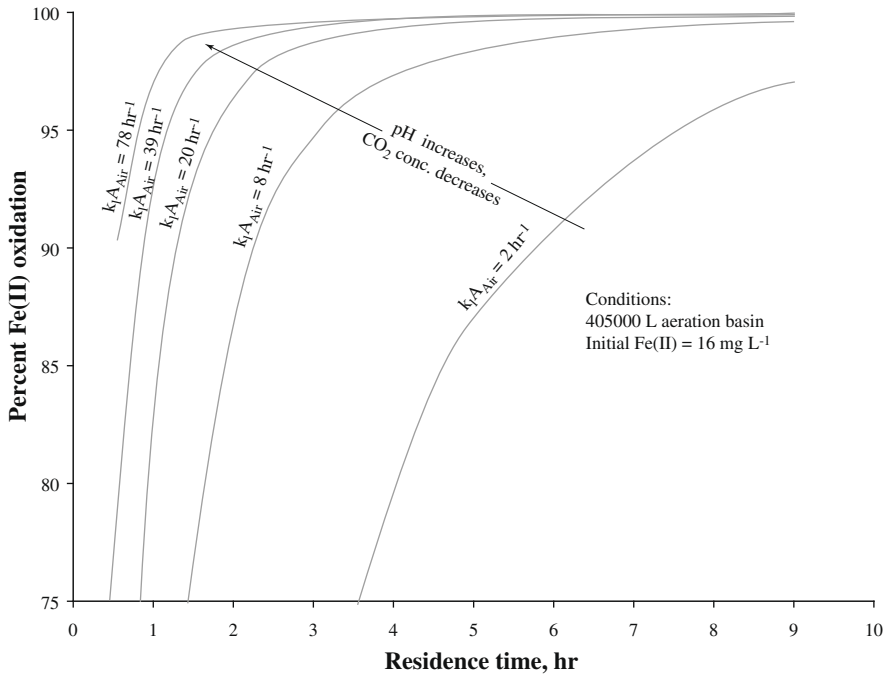

Fig. 7. Model 2 results for % Fe oxidation versus residence time for a full-scale treatment of Site 21, contoured for different mass transfer coefficients (k_lA_{Air}, governed by aeration effectiveness).

The published Fe removal rate of 20 g m^{-2} d^{-1} (Hedin et al., 1994; Watzlaf et al., 2004) has proved useful for sizing successful passive treatment systems for net-alkaline water at numerous field sites. However, the Site 21 14-L and 400-L non-aerated reactors and their flows were scaled to ponds suggested to be adequately sized using 20 g m^{-2} d^{-1}, but these experiments did not adequately oxidize Fe, showing only 16% and 22% oxidation, respectively, compared to nearly 100% oxidation from the well-aerated 14-L Site 21 and Packer 5 experiments. It is not clear how large a passive treatment system would actually need to be for the Site 21 or Packer 5 discharges. At a passive treatment wetland with similar influent water chemistry, Cravotta (2007) found only a 3.7 g m^{-2} d^{-1} removal rate for a non-aerated system that was originally designed to have aeration; experiments predicted 80–100% Fe oxidation with aeration. Results from Cravotta (2007) and this study strongly suggest that completely passive Fe removal at Site 21, Packer 5, and some other net-alkaline waters would be much slower than 20 g m^{-2} d^{-1}. The authors suggest investigation of CO_2 degassing rates before passive treatment is implemented for CO_2-rich net-alkaline mine water.

The method of aeration can have a dramatic influence on the effectiveness of treatment. Varying the mass transfer coefficient (k_lA_{Air}) can be accomplished several ways, including changing air flow rate, diffuser technology, diffuser spatial density, diffuser depth, and pond volume (surface area to volume ratio). Smaller air bubbles will provide more efficient air transfer and CO_2 degassing due to higher surface area. Fig. 7 displays Model 2 simulation results for a full-scale aeration treatment for Site 21, demonstrating that increasing retention time (by changing water flow rate or aeration basin volume) and k_lA_{Air} both increase treatment effectiveness. A treatment designer must evaluate the cost tradeoffs for increasing retention time (pond volume) versus increasing aeration.

Although there is a chemical O_2 demand for the oxidation of Fe(II), Kirby et al. (1999) showed that the Fe(II) oxidation rate is much more sensitive to pH than to O_2 concentration as long as O_2 is present in measurable concentration. It is possible for O_2 to become rate-limiting, especially in cases where the Fe(II) concentration is high. Therefore, aeration at the upflow end of a pond may successfully drive off CO_2 and temporarily increase pH, but Fe oxidation may require the placement of additional aeration devices downflow to ensure that O_2 is replenished and does not become rate-limiting.

The semi-passive treatment of net alkaline, CO_2-rich mine drainage by aeration can be an extremely effective method to rapidly oxidize Fe(II) in smaller areas than needed for completely passive treatment. Aeration can allow the oxidation pond to be 10 or more times smaller than a passive aerobic treatment pond. In either case, a settling pond or wetlands for solids removal generally would be needed downflow of the oxidation pond. However, until reliable predictions of settling rates are available, it will not be possible to determine the size and cost of the settling pond. There is also a power requirement for the aeration that will be dependent upon the flow rate, Fe(II) concentration, and method of air introduction.

Although net-alkaline CO_2-rich discharges may be less common than net-acidic discharges, many large, high-metal loading AMD sources in the anthracite and bituminous coal regions of Pennsylvania are net alkaline (e.g., Cravotta and Kirby, 2004a; Cravotta, 2005, 2008). For net-acidic AMD, anoxic limestone drains (ALD) or other limestone based systems are commonly used as the first stage of passive treatment of acidic mine drainage and, if effective, will produce net-alkaline CO_2-rich water that requires oxidation to complete its treatment. Therefore this research should prove valuable for the evaluation of treatment strategies for net-alkaline or net-acidic discharges.

Acknowledgments

We wish to thank the Pennsylvania Department of Environmental Protection Growing Greener Program for funding, Katherine Mabis McKenna Foundation for financial support of Dennis, Aeration Solutions Inc. for donation of diffusers and a blower, Shamokin Creek Restoration Alliance members for background information on Scarlift Site 21, Dr. C. A. Cravotta, III for information on the Packer 5 discharge and a thorough informal review, and M. Dennis for

field work and motivation. We thank three anonymous reviewers for their contributions to manuscript clarity.

References

American Public Health Association (APHA), 1998. Standard Methods for the Examination of Water and Wastewater, twentieth ed. American Public Health Association, Washington, DC.

Budeit, D., 2007. Role of accelerated oxidation for removal of metals from mine drainage. In: Barnhisel, R.I. (Ed.), National Meeting of the American Society of Mining and Reclamation, Gillette, WY, June 2–7.

Cravotta, III, C.A., 2005. Effects of Abandoned Coal-Mine Drainage on Streamflow and Water Quality in the Mahanoy Creek Basin, Schuylkill, Columbia, and Northumberland Counties, Pennsylvania, 2001. US Geol. Surv. Scient. Invest. Rep. 2004-5291.

Cravotta III, C.A., 2007. Passive aerobic treatment of net-alkaline, iron-laden drainage from a flooded underground anthracite mine, Pennsylvania, USA. Mine Water Environ. 26 (3), 128–149.

Cravotta III, C.A., 2008. Dissolved metals and associated constituents in abandoned coal mine discharges, Pennsylvania, USA; part 1, constituent quantities and correlations. Constituent concentrations and correlations. Appl. Geochem. 23, 166–202.

Cravotta, III, C.A., Kirby, C.S., 2004a. Effects of abandoned coal-mine drainage on streamflow and water quality in the Shamokin Creek Basin, Northumberland and Columbia Counties, Pennsylvania, 1999–2001. US Geol. Surv. Water-Resour. Invest. Rep. 03-4311.

Cravotta III, C.A., Kirby, C.S., 2004b. Acidity and alkalinity in mine drainage: Practical considerations. In: Proceedings of American Society for Mining & Reclamation Conf., Morgantown, WV, April 18–24.

Cravotta III, C.A., Dugas, D.L., Brady, K.B.C., Kovalchuk, T.E., 1994. Effects of selective handling of pyritic, acid-forming materials on the chemistry of pore gas and ground water at a reclaimed surface coal mine in Clarion Country. US Bureau of Mines Spec. Publ. SP 06A, PA, USA (pp. 365–374).

Dempsey, B.A., Roscoe, H.C., Ames, R., Hedin, R., Jeon, B.H., 2001. Ferrous oxidation chemistry in passive abiotic systems for treatment of mine drainage. Geochem. Expl. Environ. Anal. 1, 81–88.

Dietz, J.M., Dempsey, B.A., 2002. Innovative treatment of alkaline mine drainage using recirculated iron oxides in a complete mix reactor. In: Barnhisel, R.I. (Ed.), National Meeting of the American Society of Mining and Reclamation, Lexington, KY, June 9–13.

Gannett Fleming Corddry and Carpenter, Inc., 1972. Operation Scarlift Project No. SL-113: Mine Drainage Abatement Measures for the Shamokin Creek Watershed. Gannett Fleming Corddry and Carpenter, Inc. Engineers, Harrisburg, Pennsylvania, prepared for the PA Department of Environmental Resources.

Hedin, R.S., Nairn, R.W., Kleinmann, R.L.P., 1994. Passive treatment of coal mine drainage. Info. Circ. (US Bur. Mines, US Dept. Interior.), No. 9389.

Jacobson, B.A., Unz, R.F., Dempsey, B.A., 1999. An analysis of manganese as an indicator for heavy metal removal in passive treatment using laboratory spent mushroom compost columns. In: Proceedings of Sixteenth Annual National meeting of the American Society for Surface Mining and Reclamation; Mining and reclamation for the next millennium, pp. 81–90.

Jageman, T.C., Yokley, R.A., Heunisch, H.E., 1988. The use of preaeration to reduce the cost of neutralizing acid mine drainage. US Bur. Mines Information Circular IC 9183, 131–135.

Kirby, C.S., Cravotta III, C.A., 2005a. Net alkalinity and net acidity 1: theoretical considerations. Appl. Geochem. 20, 1920–1940.

Kirby, C.S., Cravotta III, C.A., 2005b. Net alkalinity and net acidity 2: practical considerations. Appl. Geochem. 20, 1941–1964.

Kirby, C.S., Thomas, H.M., Southam, G., Donald, R., 1999. Relative contributions of abiotic and biologic factors in Fe(II) oxidation in mine drainage. Appl. Geochem. 14, 511–530.

Langmuir, D., 1997. Aqueous Environmental Geochemistry. Prentice-Hall, Upper Saddle River, NJ.

Means, B., 2007. US Office of Surface Mining, Harrisburg PA, pers. comm.

Parkhurst, D.L., Appelo, C.A.J., 1999. User's guide to PHREEQC (Version 2) – a computer program for speciation, batch-reaction, one-dimensional transport, and inverse geochemical calculations. US Geol. Surv. Water-Resour. Invest. Rep. 99-4259.

Reed, L.A., Beard, M.M., Growitz, D.J., 1987. Quality of water in mines in the western middle coal field, anthracite region, east-central Pennsylvania. US Geol. Surv. Water-Resour. Invest. Rep. 64.

Rose, A.W., Cravotta III, C.A., 1998. Geochemistry of coalmine drainage. In: Brady, K.B.C., Smith, M.W., Schueck, J. (Eds.), Coal Mine Drainage Prediction and Pollution Prevention in Pennsylvania. Pennsylvania Dept. Environ. Prot. 5600-BK-DEP2256, Harrisburg, PA, pp. 1.1–1.22.

Schmidt, T., 2007. Skelly and Loy, Harrisburg PA, pers. comm.

Stumm, W., Morgan, J.J., 1996. Aquatic Chemistry: Chemical Equilibria and Rates in Natural Waters. Wiley-Interscience, New York.

Watzlaf, G.R., Schroeder, K.T., Kleinmann, R.L.P., Kairies, C.L., Nairn, R.W., 2004. The Passive Treatment of Coal Mine Drainage, DOE/NETL-2004/1202. <http://www.netl.doe.gov/technologies/coalpower/ewr/water/pdfs/Passive%20Treatment.pdf> (accessed August 2007).

Wood, C.R., 1996. Water quality of large discharges in the anthracite region of eastern Pennsylvania. US Geol. Surv. Water-Resour. Invest. Rep. 95-4243.